Development 134, 4053-4062 (2007) doi:10.1242/dev.005363

# The *C. elegans* ROR receptor tyrosine kinase, CAM-1, non-autonomously inhibits the Wnt pathway

**Jennifer L. Green, Takao Inoue and Paul W. Sternberg***

Inhibitors of Wnt signaling promote normal development and prevent cancer by restraining when and where the Wnt pathway is activated. ROR proteins, a class of Wnt-binding receptor tyrosine kinases, inhibit Wnt signaling by an unknown mechanism. To clarify how RORs inhibit the Wnt pathway, we examined the relationship between Wnts and the sole *C. elegans* ROR homolog, *cam-1*, during *C. elegans* vulval development, a Wnt-regulated process. We found that loss and overexpression of *cam-1* causes reciprocal defects in Wnt-mediated cell-fate specification. Our molecular and genetic analyses revealed that the CAM-1 extracellular domain (ECD) is sufficient to non-autonomously antagonize multiple Wnts, suggesting that the CAM-1/ROR ECD sequesters Wnts. A sequestration model is supported by our findings that the CAM-1 ECD binds to several Wnts in vitro. These results demonstrate how ROR proteins help to refine the spatial pattern of Wnt activity in a complex multicellular environment.

**KEY WORDS: ROR, CAM-1, Wnt, Vulva, Patterning, CRD, Organogenesis, Morphogen**

## INTRODUCTION

Wnt signaling is necessary for development, but causes cancer when dysregulated. The canonical Wnt pathway is initiated when a secreted Wnt glycoprotein binds to a transmembrane Frizzled (Fz) receptor and ultimately leads to β-catenin-mediated regulation of gene transcription (Logan and Nusse, 2004). The Wnt pathway is actively constrained by secreted antagonists and inhibitors of signal transducers (Kawano and Kypta, 2003; Logan and Nusse, 2004). The importance of negative regulators, both developmentally and to prevent tumorigenesis, prompted us to investigate the mechanistic activity of ROR proteins, a poorly understood class of Wnt inhibitors (Billiard et al., 2005; Forrester et al., 2004; Mikels and Nusse, 2006a; Mikels and Nusse, 2006b).

ROR proteins are conserved receptor tyrosine kinases (RTKs) characterized by an extracellular Fz domain [also called cysteine-rich-domain (CRD)], an immunoglobulin (Ig) domain, and a kringle domain (Fig. 1A). Mutations in ROR genes cause developmental defects including skeletal abnormalities in mice and humans (reviewed by Forrester, 2002). Studies of vertebrate RORs showed that the ROR CRD, like the Fz CRD (Bhanot et al., 1996), can bind to Wnts (Billiard et al., 2005; Hikasa et al., 2002; Kani et al., 2004; Mikels and Nusse, 2006a; Oishi et al., 2003). In cell culture, ROR2 abrogates expression of a canonical Wnt reporter (Billiard et al., 2005; Mikels and Nusse, 2006a); however, whether this antagonistic activity is cell-autonomous is unknown. To study how RORs modulate Wnt signaling in a multicellular environment, we investigated the function of the sole *C. elegans* ROR family member, *cam-1*.

Forrester et al. (Forrester, 2002; Forrester et al., 2004) studied CAM-1, which is equally similar to ROR1 and to ROR2, for its role in cell migration, where the CRD is required to antagonize EGL-20/WNT activity. During canal-associated neuron (CAN) migration, this CAM-1 function is cell-autonomous (Forrester et al., 1999). Although Forrester and others postulated that CAM-1 sequesters Wnts, reports that ROR2 can bind to Fz receptors (Oishi et al., 2003) raise the question of whether CAM-1/ROR inhibits Wnt signaling by interacting with the receptor or the ligand. We addressed these questions using vulva development as a model, as this process involves every *C. elegans* Wnt (*lin-44*, *cwn-1*, *egl-20*, *cwn-2* and *mom-2*) and Wnt receptor (*mig-1*, *lin-17*, *mom-5*, *cfz-2* and *lin-18*) (Gleason et al., 2006), and also because the well-characterized cellular phenotypes facilitate identification of signaling defects.

The *C. elegans* vulva comprises 22 cells generated by well-defined signaling events (reviewed by Sternberg, 2005) (Fig. 1B). The vulval cells are descendents of three vulval precursor cells (VPCs) located on the ventral surface of the worm (Sulston and Horvitz, 1977). During larval development, the VPCs are induced to divide by LIN-3 (EGF) secreted by the anchor cell (AC), (Hill and Sternberg, 1992). The VPC most proximal to the AC, P6.p, receives the most LIN-3 inductive signal through the receptor LET-23 (EGFR) (Katz et al., 1995; Yoo et al., 2004), triggering a MAP kinase cascade that induces P6.p to adopt the primary fate (1°) and produce eight vulval progeny. P5.p and P7.p receive lower levels of LIN-3 and a repressive lateral signal from P6.p mediated by LIN-12 (NOTCH) (Simske and Kim, 1995; Sternberg and Horvitz, 1989). These cells adopt the secondary fate (2°) and each produces seven vulval progeny. The remaining VPCs receive sub-threshold LIN-3 signal and adopt either the tertiary fate (3°), dividing once before fusing (P4.p, P8.p and sometimes P3.p), or the fused fate (F), fusing with the epidermis without dividing (P3.p adopts this fate half the time) (Sulston and Horvitz, 1977). A Wnt pathway involving BAR-1 (β-catenin) is required for the VPCs to be induced by LIN-3 and defective Wnt signaling frequently causes P5.p-P7.p to become 3° or F, instead of 1° or 2°, and also causes P3.p, P4.p and P8.p to become F instead of 3° (Eisenmann et al., 1998).

Because wild-type *C. elegans* development is essentially invariant, even slight deviations from the wild-type induction pattern can be detected and are informative. Worms producing fewer than 22 vulval cells are called 'underinduced' (UI) and worms producing greater than 22 vulval cells are called 'overinduced' (OI). The UI phenotype (Fig. 1D) is caused by reduced Wnt signaling or reduced

Division of Biology, California Institute of Technology, Mail Code 156-29, Pasadena, CA 91125, USA.

*Author for correspondence (e-mail: pws@caltech.edu)

**Accepted 25 August 2007**

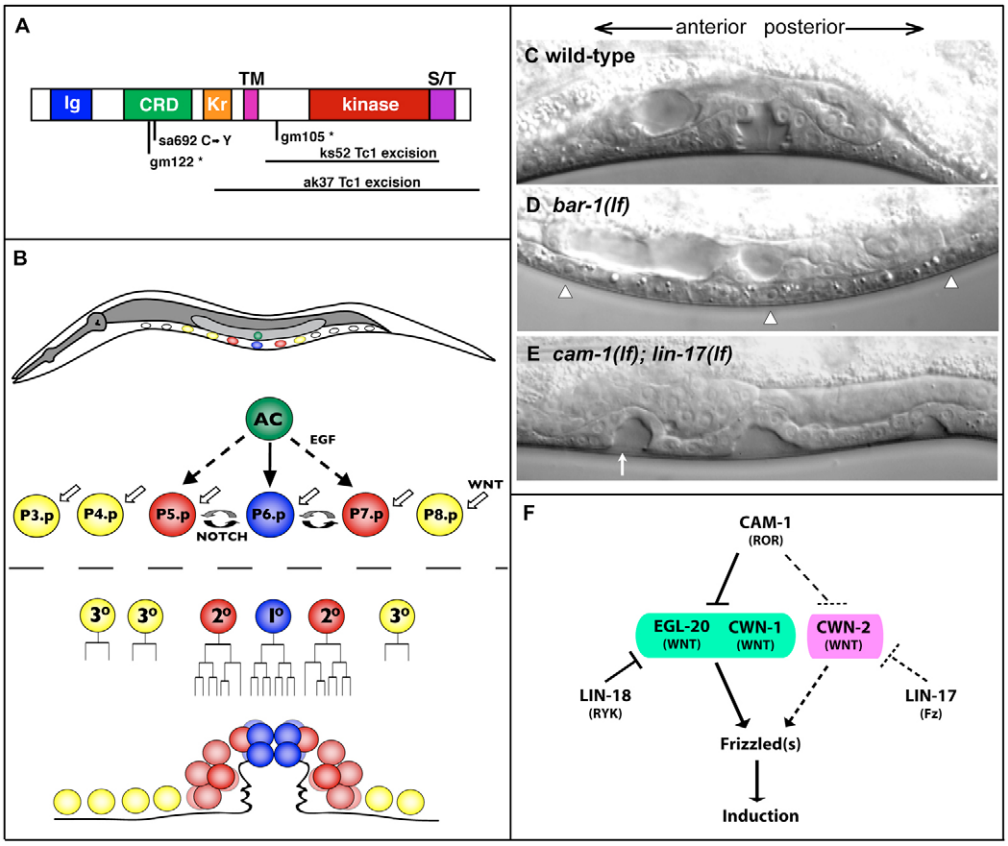


**Fig. 1. CAM-1 structure, vulval development and vulval phenotypes, and a model for CAM-1 interaction with Wnts in *C. elegans*.** (**A**) CAM-1 protein structure depicting Ig (Immunoglobulin) domain, CRD (cysteine-rich domain), Kr (kringle domain), TM (transmembrane) domain, kinase domain and S/T (serine/threonine-rich) domain. Amino terminus is to the left. Molecular lesions of *cam-1* mutant alleles are given below. (**B**) Schematic of vulval induction process. (**C-E**) Nomarski images of hermaphrodite vulvae. Anterior, left; posterior, right; dorsal, up; ventral, down. (C) Wild-type vulva formed from 22 progeny of 3 VPCs: P5.p, P6.p and P7.p. (D) A UI *bar-1(ga80)* mutant with no VPCs induced. Arrowheads point to nuclei of P5.p, P6.p and P7.p that have adopted the F fate. (E) *lin-17(n671); cam-1(gm122)* double mutant displaying an OI phenotype. Arrow points to ectopic invagination caused by induction of P4.p. (**F**) Proposed model of CAM-1 interaction with Wnts. Arrows represent positive interaction, bars negative interaction, and dashed lines a possible interaction.

Ras/MAPK signaling. The OI phenotype (Fig. 1E) is caused by increased Ras/MAPK signaling (Ferguson et al., 1987), increased lateral signaling (Greenwald et al., 1983) or increased Wnt activity (Gleason et al., 2002; Korswagen et al., 2002).

Here, we show that CAM-1 inhibits Wnt pathway activity during vulval development by limiting the levels of Wnts that interact with the VPCs. We find that expression of the CAM-1 ECD in non-vulval tissue is sufficient to limit Wnt pathway activity in the VPCs, whereas CAM-1 expression in the VPCs failed to rescue the *cam-1* mutant phenotype, suggesting a non-autonomous mode of inhibition. We also find that the CAM-1 ECD specifically binds to Wnts, supporting the model that CAM-1 sequesters Wnt ligands. Our results demonstrate how CAM-1/ROR contributes to the complex spatial profile of Wnt signaling by modifying the range of Wnt activity.

## MATERIALS AND METHODS

### Strains and genetics

*C. elegans* was handled as described previously (Brenner, 1974). All strains used are derivatives of *C. elegans* N2 Bristol strain. LG1: *lin-17(n671)*, *lin-17(n677)*, *lin-44(n1792)*, *mom-5(or57)*, *mom-5(zu193)*. LGII: *cwn-1(ok546)*, *cam-1(gm122)*, *cam-1(ks52)*, *cam-1(gm105)*, *cam-1(sa692)*, *cam-1(ak37)*, *rol-6(e187)*. LGIII: *lin-12(n952)*, *unc-119(ed4)*. LGIV: *lin-3(e1417)*, *lin-3(n378)*, *ark-1(sy247)*, *dpy-20(e1282)*, *egl-20(n585)*, *egl-20(hu120)*, *cwn-2(ok895)*. LGV: *him-5(e1490)*. *LGX: lin-18(e620)*, *bar-1(ga80)*, *gap-1(n1691)*, *unc-2(e55)*, *sli-1(sy143)*, *daf-3(mgDf90)*. For RNAi experiments, gravid hermaphrodites were fed RNAi-expressing bacteria and L4 progeny were scored.

### Vulval phenotypes

Vulval induction was scored in mid-L4 stage hermaphrodites by counting vulval cell nuclei using Nomarski DIC optics. If both VPC daughters divided, that VPC was counted as induced (1.0). If only one VPC daughter divided, that VPC was counted as half-induced (0.5). *Pmyo-3::CAM-1::GFP* displayed increased penetrance of the UI phenotype at 25°C. Thereafter, all *CAM-1::GFP* transgenic worms (except *cwEx164*) were grown at 25°C. All other strains were grown at 20°C.

### Contributions of LIN-17 and MOM-5 to vulval induction

Our results are inconsistent with the positive role for LIN-17 in vulva induction reported by Gleason et al. (Gleason et al., 2006). Whereas Gleason et al. report that 12% of *lin-17(n671)* worms are UI, we did not observe any UI *lin-17(n671)* worms. To address this discrepancy we obtained *lin-17(n671)* worms used by Gleason et al. from the Eisenmann laboratory (*–DE*) and did not detect any UI worms (see Table S2 in the supplementary material). By contrast, we observed one *lin-17(n671)-DE* worm that was OI and had five VPCs induced (see Fig. S1 in the supplementary material). Our examination of *mig-1(e1787); lin-17(n671)* and *lin-17(n671); cfz-2(ok1201)* double mutants did not reveal a UI phenotype. Also, *lin-17(lf)* did not enhance the UI phenotype of *cwn-1(lf)* mutant worms. *lin-17(n671)-DE;*

*cam-1(lf)* double-mutant worms recapitulated the synthetic OI phenotype, as did double mutants containing another *lin-17* allele, *n677*. The elevated Wnt signaling observed in the *lin-17(lf); cam-1(lf)* background, which cannot be explained by signaling through LIN-17, is likely to be due to increased signaling through another Frizzled receptor, such as MOM-5. Thus, we examined vulval induction in *mom-5* mutants (see Table S2 in the supplementary material). In contrast to *lin-17*, we found that mutation of *mom-5* caused a dramatic UI phenotype, suggesting that *mom-5*, but not *lin-17*, is required for vulval induction.

### Transgenics

Extrachromosomal arrays were generated by co-injecting *CAM-1b::GFP* driven by various promoters with *unc-119 (+)* (60 ng/μL) into *unc-119(ed4)* hermaphrodites as described (Mello et al., 1991). Of the three *cam-1* splice variants, the 'b' isoform was selected because it appears to have a weak signal sequence, whereas the 'a' and 'c' variants have no detectable signal sequence. *cam-1* tissue-specific constructs were made by shuttling various promoters upstream of *CAM-1b::GFP* using 5′ *Bam*HI and 3′ *Not*I sites. All constructs were injected at 50 ng/μL except *syEx863*, *syEx864*, and *syIs198*, which were injected at 75 ng/μL. To facilitate examination of *Pcam-1::CAM-1::GFP* and *Pcam-1::CAM-1ΔIgKriIntra::GFP*, *dpy-20(e1282)* was crossed into strains WF1863 and WF1729, respectively (Forrester et al., 1999; Kim and Forrester, 2003) to suppress the roller phenotype. *syIs75(Plin-18::LIN-18::GFP)* is an integrated line of *syEx363[pTI00.43(60ng/μl) + unc-119 (+)(30ng/μl)]* (Inoue et al., 2004). *syEx1022[LIN-17::GFP(40ng/μl) + unc-119(+)(90ng/μl) + myo-2::DsRed(15ng/μl)]* was made with plasmid *PSH22* (gift from H. Sawa, RIKEN, Kobe, Japan). *syEx1020[Pmyo-3::LIN-17::GFP(50ng/μl) + unc-119(+)(90ng/μl) + Pmyo-2::DsRed(15ng/μl)]* contains a *Pmyo-3::LIN-17::GFP* plasmid that was made by amplifying the N-terminal-encoding portion of *lin-17* from PSH22 (forward primer, TCCATCTAGAGGCTCCTTCTCCAAAATGATGCATTCTTTGGGC; reverse primer, GCACAATGCGACTTGGGATCGTGTGG). The *lin-17* C-terminal-encoding portion was amplified from cDNA (forward primer, CCAAGCCAACCGGGTGCCCCAG; reverse primer, TCTTCCGGAACGACCTTACTGGGTCTCCATGAATTCTG). The C-terminal-encoding portion was cleaved by *Bam*HI and *Bsp*EI and transferred into Fire vector L4817 (*Pmyo-3*) that had been cleaved by *Age*I and *Bam*HI. The N-terminal-encoding portion was then cleaved by *Xba*I (cuts twice) and *Bam*HI. The *Xba*I-*Bam*HI fragment was transferred in first, followed by the *Xba*I-*Xba*I fragment.

### Generating the *CAM-1b::GFP* backbone

To make the *CAM-1b::GFP* backbone, C01G6.8a cDNA was first inserted into Fire vector pPD49.83 using the *Nhe*I site. To create *hs::CAM-1::GFP*, *Bsp*EI and *Apa*I sites were used to switch the 3′ end of *cam-1* with the 3′ end of *CAM-1::GFP* from plasmid pMini3 (gift from W. Forrester, Indiana University, Bloomington, IN) which also includes the last two small introns of *cam-1*. Next, the 5′ end of C01G6.8b was amplified from cDNA using forward primer ATAAGATGCGGCCGCATGGAGGGTACATCAACTGGTCAACG to add a *Not*I site to the 5′ end (reverse primer TTCCAATGCATTGGCATCTAGCCATCGTTCTGATACAGC). The C01G6.8b 5′ end was then cloned into pBluescript using *Not*I and *Bst*XI and transferred into *hs::CAM-1::GFP* using *Bam*HI and *Bst*EII, creating *CAM-1b::GFP* with a *Not*I site 5′ of the ATG.

### Tissue-specific constructs

*syEx778*, *syEx781* and *syEx814* contain 2.4 kb of *Pmyo-3* (*myo-3* 5′ regulatory region) amplified from Fire vector L4817 with forward primer CGCGGATCCGGTCGGCTATAATAAGTTCTTGAATA and reverse primer ATAGTTTAGCGGCCTCTAGATGGATCTAGTGGTCGTG. *syEx798* and *syEx799* contain 3.4 kb of *Pdpy-8* amplified from genomic DNA using forward primer CGCGGATCCGAACTGAGAATGCTGACGGATG and reverse primer ATAGTTTAGCGGCCGATGGGAAAATAAGAAAAGGAAATGTGG. *syEx863* and *syEx864* contain 5.5 kb of *Psur-2* amplified from cosmid F39B2 using forward primer CGCGGATCCCGAAATTCGGTAGATTTGGGC and reverse primer ATAGTTTAGCGGCCGCTTGTTGCCTGAAAATGTAATAATTTTC. *syEx780* and *syEx777* contain 4.9 kb of *Pfos-1a* amplified from plasmid pDRS46 (Sherwood and Sternberg, 2003) using forward primer CGCGGATCCTGGGCAGCTGTAAAACGTCTTTAC and reverse primer ATAGTTTAGCGGCCTCCACTCTCTTATATAGCAGAGGTG. *syEx775* and *syEx776* contain 3 kb of *Psnb-1* amplified from plasmid *Psnb-1::slo-1* (Davies et al., 2003) using forward primer CGCGGATCCAAGCTTTTTGCTGAAATCTAGGATTAC and reverse primer ATAGTTTAGCGGCCGCTGTTCCCTGAAATGAAGCGA. *syIs198* contains 1.6 kb of *Plst-1* amplified from plasmid *lst-1p-gfp-lacZ* (gift from Iva Greenwald c/o Andrew Yoo, Howard Hughes Medical Institute, Columbia University, NY) using forward primer CGCGGATCCCAATTGTTACTACTGACGGCATTCC and reverse primer ATAGTTTAGCGGCCGCGTCAAATAATTCTTTTGAAATGAGAAAGAACTTGGC. To make *Pmyo-3::CAM-1ΔIntra::GFP*, blunt *Hpa*I and *Msc*I sites were used to switch the C-terminus-encoding part of *Pmyo-3::CAM-1b::GFP* with a *Hpa*I-*Hpa*I fragment (10.8 kb) from pDM108 (Francis et al., 2005) that contains *cam-1* minus the sequence encoding the kinase domain (removal of C-terminal 346 codons), fused to *GFP*.

### Immunoblotting

Lysates of transfected and untransfected *Drosophila* S2 cells were run on a 4-12% NuPAGE Bis-Tris gel (Invitrogen) and probed with anti-HA monoclonal antibody G036 (Applied Biological Materials, Vancouver, BC) or polyclonal anti-GAPDH (Sullivan et al., 2003).

### Reverse binding assay

The CRD-AP fusion proteins were made in 293T cells as previously described for *Drosophila* CRD-AP fusions (Wu and Nusse, 2002). The CRD of the sFRP3-AP fusion was replaced with the CRD (or WIF) of *C. elegans* receptors. Each construct contains sFRP3 signal sequence, *C. elegans* CRD (or WIF), C-terminal domain of sFRP3 and AP. Sequences across the signal sequence fusion junction are (CRD/WIF underlined): CAM-1, PGAQAAGSNYAPVA; LIN-18, PGAQANVNMFISK; LIN-17, PGAQASIFDQAVKG; MOM-5, PGAQADQRLSSTSI; CFZ-2, PGAQALFGKRQKCE; MIG-1, PGAQAQRCQKVDHE. Downstream fusion junctions are (CRD/WIF domains underlined): CAM-1, STSNCIHALAIVTAD; LIN-18, TDSIDKTRALAIVTAD; LIN-17, PPELCMNALAIVTAD; MOM-5, VTDLCVDALAIVTAD; CFZ-2, TGNICADALAIVTAD; MIG-1, NREKMCMNALAIVTAD. To determine the concentration of CRD-AP fusion protein in the conditioned medium, we immunoprecipitated the CRD-AP fusion proteins with anti-AP antibody (Sigma A-2951), resolved the immunocomplexes by SDS-PAGE and estimated the protein concentration after staining with Coomassie Blue. Activities of the CRD-AP fusion proteins were assayed colorimetrically after incubation with the AP substrate. Each of the CRD-AP fusion proteins was determined to have similar specific activity of 3 pmol/unit activity. The protein was concentrated by ammonium sulfate precipitation (3.2 M) followed by dialysis against Hank's Balanced Salt Solution without calcium and magnesium (HBSS) and the samples were then normalized by AP activity. The Neurotactin (Nrt)-HA-Wnt fusion proteins were made as previously described for *Drosophila* Nrt-HA-Wnt fusions (Wu and Nusse, 2002) with the exception that we used the pCoBlast selection vector (Invitrogen) and 25 μg/mL blasticidin for selection. The sequences around the regions linking HA and the Wnts are (Wnt sequences underlined): Nrt-CWN-1, WEDEEASLAANRFD; Nrt-CWN-2, WEDEEASLNVQSLL; Nrt-EL-20, WEDEEASPSATYST and WEDEEASGHNVKP; Nrt-MOM-2, WEDEEASKSADAWW; Nrt-LIN-44, WEDEEASAPAGKIV. The binding assay protocol was adapted from those previously published (Cheng and Flanagan, 1994; Flanagan and Leder, 1990; Wu and Nusse, 2002). We observed that Nrt-HA-Wnt expression appeared to decrease with time as cells were passaged. Because of this observation and the non-clonality of the stable lines, we performed the binding assays as soon as sufficient cell numbers had recovered from antibiotic selection and used equal cell numbers for the assay rather than normalizing to levels of Wnt expression. S2 cells stably transfected with the Nrt-HA-Wnt fusion constructs were counted with a hemacytometer and then heat shocked for 45 minutes at 37°C followed by 2 hours incubation at 25°C. At this point, aliquots of 500,000 cells were frozen for western analysis. The remaining cells were then resuspended in HBSS plus 10% BSA and incubated with CRD-AP ($7\times10^{-8}$ M) in Eppendorf tubes for 90 minutes at 25°C. Three binding reactions of 30,000 cells each were performed for 26

of 30 combinations. For the remaining four combinations (MIG-1, MOM-5 and CFZ-2 CRDs with untransfected S2 cells, and LIN-18 CRD with Nrt-HA-LIN-44-expressing cells), only two reactions of 30,000 cells each were performed. After washing cells three times with HBSS, cells were lysed by adding HBSS plus 1% Triton X-100 with brief vortexing and then heated at 70°C for 10 minutes to kill background phosphatase activity. Supernatant was transferred to a 96-well untreated microtiter plate and incubated with the chromogenic substrate p-nitrophenyl phosphate (Sigma N-7653). After 24 hours the absorbance was read at 405 nm using a microtiter plate spectrophotometer (Bio-Rad) (for raw data see Table S3 in the supplementary material).

## RESULTS

### CAM-1 negatively regulates vulval induction

To study how CAM-1/ROR inhibits Wnt signaling, we investigated the role of CAM-1 in vulval development, a process requiring multiple Wnts. None of the five *cam-1* alleles tested (Fig. 1A) caused induction defects (Table 1). However, as vulval development requires several redundant Wnts and receptors (Gleason et al., 2006), we looked for genetic interactions between *cam-1* and Wnt receptors *lin-17/Frizzled* (Sawa et al., 1996) and *lin-18/Ryk* (Inoue et al., 2004). We found that worms doubly mutant for *cam-1* and loss-of-function (lf) mutations in *lin-17* or *lin-18* displayed an OI phenotype (greater than 22 vulval cells). *lin-17(lf)* and *lin-18(lf)* mutants frequently display a polarity defect in the P7.p lineage that is distinct from vulval induction. This polarity defect alters the arrangement, but not the number, of vulval cells. To distinguish between induction defects and polarity defects, we counted the vulval nuclei. Both *lin-17(lf)* and *lin-18(lf)* animals had the wild-type pattern of 3-cell induction; P6.p adopted the 1° fate, P5.p and P7.p adopted the 2° fate, and the remaining VPCs were not induced. We found that 17% of *lin-17(lf); cam-1(lf)* double mutants and 12% of *cam-1(lf); lin-18(lf)* double mutants were OI (Table 1, Fig. 1E), with either 3.5, 4.0 or 4.5 VPCs induced. Since neither *lin-17(lf)* nor *lin-18(lf)* single mutants were OI, these results suggest that CAM-1 negatively regulates vulval induction and that *lin-17(lf)* and *lin-18(lf)* provide a sensitized background in which to observe CAM-1 function. To determine whether the OI phenotype is a common phenotype among *cam-1; Fz* double mutants, we constructed worms doubly mutant for *cam-1(lf)* and two other Fz receptors, *mig-1* and *cfz-2*. 0/21 *mig-1(lf); cam-1(lf)* and 1/22 *cam-1(lf); cfz-2(lf)* double-mutant worms were OI, indicating that sensitization is specific to *lin-17*.

**Table 1. CAM-1 inhibits vulval development**

| Genotype | % OI* | % UI† | Average no. of VPCs induced | *n* | *P* value‡ |
|---|---|---|---|---|---|
| + | 0 | 0 | 3.00 | Many | |
| *cam-1(gm122)* | 2 | 0 | 3.01±0.01 | 55 | |
| *cam-1(sa692)* | 2 | 0 | 3.02±0.02 | 51 | |
| *cam-1(ak37)* | 0 | 0 | 3.00±0.00 | 53 | |
| *cam-1(gm105)* | 0 | 0 | 3.00±0.00 | 54 | |
| *cam-1(ks52)* | 0 | 0 | 3.00±0.00 | 53 | |
| *lin-17(n671)* | 0 | 0 | 3.00±0.00 | 113 | |
| *lin-17(n671); cam-1(gm122)* | 17 | 0 | 3.13±0.04 | 52 | **<0.0001**§ |
| *lin-17(n671); cam-1(sa692)* | 14 | 0 | 3.09±0.04 | 51 | **0.0007**§ |
| *lin-17(n671); cam-1(ak37)* | 14 | 0 | 3.12±0.04 | 56 | **0.0003**§ |
| *lin-17(n671); cam-1(gm105)* | 8 | 0 | 3.02±0.02 | 52 | Not sig.§ |
| *lin-17(n671); cam-1(ks52)* | 0 | 2 | 2.98±0.02 | 53 | Not sig.§ |
| *lin-17(n671); cam-1(gm122); cam-1 RNAi* | 15 | 0 | 3.11±0.06 | 27 | |
| *lin-17(n671); cam-1 RNAi* | 8 | 0 | 3.08±0.06 | 25 | **0.03**§ |
| *lin-18(e620)* | 0 | 0 | 3.00±0.00 | 113 | |
| *cam-1(gm122); lin-18(e620)* | 12 | 0 | 3.09±0.04 | 52 | **0.0008**¶ |
| *cam-1(sa692); lin-18(e620)* | 10 | 4 | 3.03±0.04 | 54 | **0.0101**¶ |
| *cam-1(ak37); lin-18(e620)* | 4 | 0 | 3.03±0.02 | 51 | Not sig.¶ |
| *cam-1(gm105); lin-18(e620)* | 0 | 0 | 3.00±0.00 | 53 | Not sig.¶ |
| *cam-1(ks52); lin-18(e620)* | 0 | 0 | 3.00±0.00 | 53 | Not sig.¶ |
| *cwn-1(ok546)* | 0 | 13 | 2.87±0.04 | 62 | |
| *cwn-2(ok895)* | 0 | 0 | 3.00±0.00 | 58 | |
| *egl-20(n585)* | 0 | 0 | 3.00±0.00 | 51 | |
| *egl-20(hu120)* | 0 | 8 | 2.92±0.04 | 50 | |
| *cwn-1(ok546); cwn-2(ok895)* | 0 | 27 | 2.68±0.09 | 44 | |
| *cwn-1(ok546); egl-20(n585)* | 0 | 84 | 1.52±0.13 | 61 | |
| *lin-17(n671); cwn-1(ok546); cam-1(gm122)* | 8 | 12 | 2.92±0.07 | 50 | Not sig.** |
| *lin-17(n671); cam-1(gm122); cwn-2(ok895)* | 4 | 0 | 3.04±0.03 | 50 | 0.052** |
| *lin-17(n671); cam-1(gm122); egl-20(n585)* | 18 | 4 | 3.12±0.06 | 51 | Not sig.** |
| *cwn-1(ok546); cam-1(gm122); lin-18(e620)* | 0 | 13 | 2.83±0.07 | 53 | **0.013**†† |
| *cam-1(gm122); cwn-2(ok895); lin-18(e620)* | 6 | 0 | 3.06±0.03 | 53 | Not sig†† |
| *cam-1(gm122); egl-20(n585); lin-18(e620)* | 0 | 10 | 2.91±0.04 | 50 | **0.027**†† |
| *lin-17(n671); cam-1(gm122); syIs198[Plst-1::CAM-1::GFP]* | 8 | 3 | 2.99±0.09‡‡ | 38 | Not sig.** |

Worms were grown and scored 20°C. Induced values are mean±s.e.m.
*OI animals are those with greater than three VPCs induced.
†UI animals are those with fewer than three VPCs induced.
‡*P* values were calculated using Fisher's exact test, comparing the fraction of worms that are Muv versus not Muv.
*P*<0.05 considered significant and represented by bold type. §Compared with *lin-17(n671)*; ¶compared with *lin-18(e620)*; **compared with *cam-1(gm122); lin-17(n671)*; ††compared with *cam-1(gm122); lin-18(e620)*.
‡‡1 out of 38 worms was UI. This worm had 0 VPCs induced and appeared to be missing the anchor cell.

## Analysis of CAM-1 domains and site of action

We analyzed the five available *cam-1* alleles (Fig. 1A) in combination with *lin-17(lf)* and *lin-18(lf)* (Table 1). The *cam-1* alleles that caused an OI phenotype are either null (*gm122*) (Forrester et al., 1999), disrupt the CRD (*sa692*) (Ailion and Thomas, 2003; Kim and Forrester, 2003), or disrupt the insertion of the ECD into the membrane (*ak37*) (Francis et al., 2005). By contrast, an allele truncating most of the intracellular domain (*gm105*) (Forrester et al., 1999), and an allele eliminating the kinase domain (*ks52*) (Koga et al., 1999), did not cause increased vulval induction. Analysis of these alleles provides structure-function information about CAM-1. Since the *sa692* allele eliminates a conserved cysteine in the CRD (Wnt-binding) domain, negative regulation of vulval development by CAM-1 requires membrane-insertion of the ECD containing the CRD, but does not require the intracellular domain. RNAi of *cam-1* in *lin-17(lf)* worms recapitulated the OI phenotype and *cam-1* RNAi of *cam-1(lf); lin-17(lf)* worms did not reduce the OI phenotype, confirming that the OI phenotype is due to reduced CAM-1 activity and not to a neomorphic function of mutant *cam-1*.

*cam-1* expression has been reported in muscle and neurons (Forrester et al., 1999; Koga et al., 1999). We detected additional expression in the VPCs in a previously characterized *Pcam-1::CAM-1::GFP* strain, WF1863 (Forrester et al., 1999) (see Fig. 3A). To test whether *cam-1* acts in the VPCs, we tried to rescue the *lin-17(lf); cam-1(lf)* OI phenotype with an integrated VPC-specific *CAM-1::GFP* transgene driven by the *lst-1* promoter (Yoo et al., 2004). Although *Plst-1::CAM-1::GFP* was expressed in the relevant VPCs (see Fig. 3G), it failed to rescue the OI phenotype suggesting that CAM-1 is required in other tissues to negatively regulate vulval induction.

## CAM-1 interacts with genes required for vulval induction

To investigate the signaling involved in CAM-1 inhibition of vulval induction, we first tested whether the synthetic OI phenotype is dependent on the inductive LIN-3 signal. Removing the source of LIN-3 (the AC) by laser ablation of the gonadal primordium eliminates inductive Ras/MAPK signaling. In gonad-ablated wild-type worms, no VPCs are induced (Kimble, 1981; Sulston and White, 1980). Mutations that strongly activate Ras/MAPK signaling can rescue the UI phenotype caused by gonad ablation (Han and Sternberg, 1990). We ablated the gonad in wild-type and *lin-17(lf); cam-1(lf)* worms and found that vulval induction in *lin-17(lf); cam-1(lf)* worms was gonad-dependent: all 16 ablated animals had no VPCs induced. Because only strong activation of the Ras/MAPK pathway can rescue vulval induction in gonad-ablated worms, we next tested whether *cam-1(lf)* affects induction in worms with mildly reduced LIN-3 activity. *cam-1(lf)* suppressed the UI phenotype of two reduction-of-function (rf) *lin-3* alleles (see Table S1 in the supplementary material), suggesting that *cam-1* acts downstream of, or parallel to, *lin-3*. We then tested for a genetic interaction between *cam-1* and inhibitors of Ras/MAPK signaling, *ark-1*, *sli-1* and *gap-1* (Sternberg, 2005; Sundaram, 2006), which are each silent when mutated singly, but are OI (30-90%) when combined with loss of another negative regulator (Hopper et al., 2000; Yoon et al., 2000). We found no interaction of *cam-1(lf)* with mutations in *ark-1*, *sli-1* or *gap-1*, indicating that CAM-1 is probably not a negative regulator of the Ras/MAPK pathway. *lin-17(lf); gap-1(n1691)* worms were not OI, thus providing further support that loss of CAM-1 does not cause increased Ras/MAPK signaling. Besides Ras/MAPK signaling, Wnt signaling is also required for vulval induction and can cause OI phenotypes when hyperactivated (Gleason et al., 2002). Mutations in *bar-1/β-catenin* cause a UI phenotype (Eisenmann, 2005; Eisenmann et al., 1998). In contrast to the suppression we observed upon reduced activity of the Ras/MAPK pathway, *cam-1(lf)* did not suppress the UI phenotype of *bar-1(lf)*, consistent with *cam-1* and *bar-1* functioning in the same pathway.

*cam-1* mutants have a withered tail (Wit) phenotype that might position some VPCs closer to the AC and thus increase the local concentration of inductive LIN-3 signal. To investigate whether the OI phenotype is a consequence of increased VPC proximity to the AC, we tested the ability of *cam-1* to affect vulval induction independently of the AC. To do this, we used a gain-of-function (gf) allele of *lin-12/Notch*. When heterozygous, the *lin-12(n952gf)* allele causes gonad-independent specification of 2° lineages in P3.p-P8.p. As *lin-12(gf)/+* also causes loss of the AC, this phenotype is due to increased lateral signaling rather than increased Ras/MAPK signaling. We found that *cam-1(lf)* increased induction in *lin-12(gf)/+* worms (see Table S2 in the supplementary material). Thus, the effect of *cam-1(lf)* on vulval induction cannot be attributed to mispositioning of the VPCs closer to the AC, which is absent in these worms.

Starvation and passage through dauer, an alternate third larval stage usually entered under conditions of starvation or high temperature (Savage-Dunn, 2005), can affect vulval induction (Ferguson and Horvitz, 1985) and *cam-1* mutants are dauer constitutive (Daf-c) (Forrester et al., 1998; Koga et al., 1999). To test whether the OI phenotype we observe is due to passage through dauer, we constructed *lin-17(lf); cam-1(lf); daf-3(lf)* triple mutants. Although *daf-3(lf)* suppresses the Daf-c phenotype of *cam-1(lf)* (Koga et al., 1999), it did not suppress the OI phenotype of *lin-17(lf); cam-1(lf)* double mutants (see Table S1 in the supplementary material), indicating that the OI phenotype is not due to passage through dauer.

## CAM-1 antagonizes Wnts

Previous studies of CAN migration demonstrated that CAM-1 inhibits EGL-20/WNT function (Forrester et al., 2004). To determine if this is also the role of CAM-1 in vulval induction, we tested whether a strong rf mutation in *egl-20* (Harris et al., 1996) could suppress the OI phenotype of *lin-17(lf); cam-1(lf)* or *cam-1(lf); lin-18(lf)* double mutants (Table 1). *egl-20(rf)* fully suppressed the OI phenotype of *cam-1(lf); lin-18(lf)* worms indicating that the OI phenotype of these worms depends on EGL-20. However, we found that *lin-17(lf); cam-1(lf); egl-20(rf)* triple mutants were still OI (Table 1), indicating that the OI phenotype of these worms is not dependent on EGL-20. The role of CAM-1 in vulval induction is thus only partly attributed to inhibition of EGL-20 activity.

Of the five Wnts, EGL-20, CWN-1 and CWN-2 strongly promote vulval induction (Gleason et al., 2006) (Table 1). To investigate whether *cam-1(lf)* causes increased CWN-1 or CWN-2 activity, we tested the ability of mutations in these Wnt genes to suppress the OI phenotype of *lin-17(lf); cam-1(lf)* or *cam-1(lf); lin-18(lf)* double mutants. We found that *cwn-1(lf)* suppressed the OI phenotype of *cam-1(lf); lin-18(lf)* mutant worms and that *cwn-2(lf)* weakly suppressed the OI phenotype of *lin-17(lf); cam-1(lf)* mutant worms. These results indicate that *cam-1(lf)* increases the activity of CWN-1, EGL-20 and possibly CWN-2 (Fig. 1F). The inability of *cwn-1(lf)*, *egl-20(rf)*, or *cwn-2(lf)* to fully suppress the OI phenotype of *lin-17(lf); cam-1(lf)* worms suggests that the OI phenotype in this strain is caused either by one of the remaining Wnts or by multiple Wnts. In some cases, mutation of a Wnt reduced the level of

induction in *lin-17(lf); cam-1(lf)* or *cam-1(lf); lin-18(lf)* double mutants to below that of wild type, consistent with the role of these Wnts in vulval induction.

LIN-17 and LIN-18 function as typical Wnt receptors in P7.p polarity. We speculate that in addition, loss of LIN-17 and LIN-18 increases levels of extracellular Wnt and that loss of CAM-1 further increases these levels, crossing the threshold to induce the VPCs (Fig. 1F). This hypothesis is consistent with observations in the *Drosophila* wing where clones mutant for Frizzleds *fz* and *fz2* have increased extracellular levels of Wingless (Wnt) (Han et al., 2005). This increase might be caused by reduced endocytosis of ligand-bound receptor. We thus tested whether worms lacking both *lin-17* and *lin-18* display an OI phenotype. Of 51 *lin-17(lf); lin-18(lf)* double-mutant worms observed, only one displayed an OI phenotype (see Table S2 and Fig. S1 in the supplementary material). However, it is possible that the class of Wnts elevated by removal of CAM-1 complements those elevated by removal of LIN-17 and LIN-18, but the Wnts elevated by removal of LIN-17 and LIN-18 do not complement each other. Another possibility is that removal of *lin-17* or *lin-18* only mildly increases extracellular Wnt levels and that these levels do not cross the threshold unless *cam-1*, a more important regulator of Wnt levels, is also removed. We next tested whether overexpression of LIN-17 and LIN-18 might reduce extracellular Wnt levels and cause a UI phenotype. *Plin-18::LIN-18::GFP* (Inoue et al., 2004) caused a weak UI phenotype (see Table S2 in the supplementary material) and significantly increased the fraction of *cwn-1(lf)* worms with a more severe UI phenotype (<2 VPCs induced), consistent with the hypothesis that *lin-18* expression affects extracellular Wnt levels. Although transgenes can sometimes decrease gene expression by titrating out transcriptional activators (Gill and Ptashne, 1988), it is unlikely that the phenotype we see here is caused by reduced *lin-18* expression because *Plin-18::LIN-18::GFP* is an overexpression construct (not a promoter::GFP array) and rescues the *lin-18(lf)* phenotype (Inoue et al., 2004). However, we cannot rule out the possibility that the phenotype is due to promoter effects on a different gene. In contrast to *Plin-18::LIN-18::GFP*, *Plin-17::LIN-17::GFP* did not affect vulval induction; however, *Plin-17::LIN-17::GFP* caused a mild, though not statistically significant, increase in the fraction of UI *cwn-1(lf)* worms. Again, it is unlikely that this phenotype is caused by promoter effects on *lin-17* expression because *Plin-17::LIN-17::GFP* rescued the P7.p polarity defect of *lin-17(lf)* worms (data not shown). Also, loss of *lin-17* did not increase the fraction of UI *cwn-1(lf)* worms (see Materials and methods and Table S2 in the supplementary material). As with *lin-18* overexpression, we cannot rule out the possibility that the phenotype is due to promoter effects on a different gene. Because *Plin-17::LIN-17::GFP* displays a more restricted expression pattern than *Plin-18::LIN-18::GFP*, we expressed LIN-17 in body wall muscle using the *myo-3* promoter (Okkema et al., 1993). *Pmyo-3::LIN-17::GFP* did not significantly affect vulval induction, nor did it enhance the UI phenotype of *cwn-1(lf)* worms. Although the mechanism by which *lin-17* and *lin-18* mutations provide a sensitized background for *cam-1* effects on vulval induction is unclear, the role of *cam-1* as an inhibitor of vulval induction is confirmed by other experiments not dependent on *lin-17* or *lin-18* mutants (e.g. *cam-1(lf); lin-3(rf)*, *cam-1(lf); lin-12(gf/+)* see above).

## The CAM-1 ECD binds to Wnts CWN-1, EGL-20 and MOM-2

Our data suggest that non-vulval CAM-1 normally antagonizes Wnt signaling by a mechanism dependent on the CAM-1 ECD, possibly by directly binding to and impeding Wnts. Detecting association of the CAM-1 ECD with Wnts by co-immunoprecipitation experiments was impractical owing to the characteristic insolubility of Wnt proteins and the lack of available recombinant *C. elegans* Wnts. To circumvent these obstacles, we employed a reverse binding assay (Rulifson et al., 2000; Wu and Nusse, 2002) in which *C. elegans* Wnts are expressed in stably transfected insect cells and tethered to the membrane by N-terminal fusion to Neurotactin (Nrt) (Fig. 2A). Binding is determined by measuring the alkaline phosphatase (AP) activity retained by the cells after incubation with

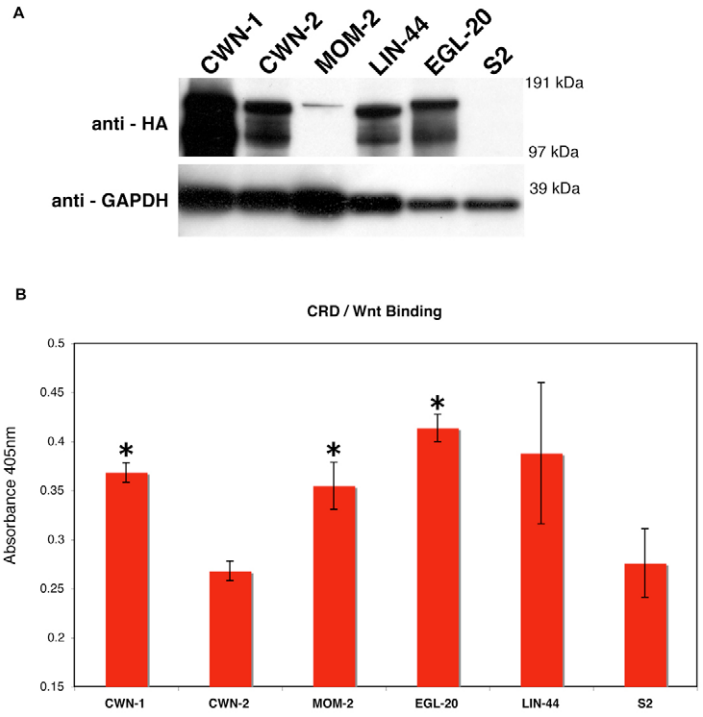


**Fig. 2. CAM-1 CRD binds Wnts CWN-1, EGL-20 and MOM-2.** *Drosophila* S2 cells expressing Neurotactin (Nrt)-HA-tagged *C. elegans* Wnts were incubated with secreted CRDs of *C. elegans* Wnt receptors fused to alkaline phosphatase (CRD-AP). (**A**) Levels of Nrt-HA-Wnt fusion proteins (~130 kD) expressed by S2 cells were measured by anti-HA immunoblot. Wnts are post-translationally modified and this might account for the detection of multiple bands. Anti-GAPDH provided a loading control. (**B**) Amount of CAM-1 CRD-AP retained by Nrt-HA-Wnt-expressing S2 cells. The assay was performed in triplicate. As the untransfected sample appeared to contain slightly fewer cells, we used cells expressing Nrt-CWN-2 (which expressed Wnt, but did not bind CAM-1 CRD-AP) as a negative control for statistical analysis. *, $P<0.05$, calculated using Fisher's exact test. Error bars, s.e.m.

secreted CAM-1 CRD-AP fusion proteins. As an internal control we assayed all combinations of *C. elegans* Wnts and Wnt receptors. This set included five Wnts (LIN-44, CWN-1, EGL-20, CWN-2, MOM-2), four Fz receptors (MIG-1, LIN-17, MOM-5, CFZ-2), and two RTKs (CAM-1/ROR, LIN-18/RYK) and confirmed that no Wnt bound indiscriminately to all receptors (see Table S3 in the supplementary material). Consistent with our genetic data, we found that the CAM-1 CRD bound to CWN-1 and EGL-20 to a significantly greater extent than to control cells (Fig. 2B). The CAM-1 CRD also bound significantly to cells expressing Nrt-MOM-2.

## Overexpression of CAM-1 non-autonomously inhibits vulval induction

If CAM-1 negatively regulates Wnt signaling by binding to and impeding Wnts, then overexpression of CAM-1 in non-vulval tissue might cause a UI phenotype. To test this, we made full-length *CAM-1::GFP* translational fusions driven by the tissue-specific promoters *Psnb-1* (pan-neuronal) (Nonet et al., 1998), *Pmyo-3* (muscle) (Okkema et al., 1993), *Pdpy-8* (epidermis), *Plin-31*(VPCs) (Tan et al., 1998), *Psur-2* (VPCs) (Singh and Han, 1995), *Plst-1* (VPCs) (Yoo et al., 2004) and *Pfos-1a* (somatic gonad) (Sherwood and Sternberg, 2003) (Fig. 3). We observed membrane-localized GFP in the expected tissues for all lines except *Plin-31*, in which we were unable to detect fluorescence. We found that expression of *CAM-1::GFP* in body wall muscle (*myo-3* promoter) and in neurons (*snb-1* promoter) caused a UI phenotype (Table 2) similar to loss of *bar-1/β-catenin* and Wnt genes: specifically, P3.p adopted the F fate at an increased frequency, P4.p was often F instead of 3°, and P5.p occasionally adopted the F or 3° fate instead of the normal 2° fate. Also similar to the consequences of mutations in Wnt pathway components, both *Pmyo-3::CAM-1::GFP* and *Psnb-1::CAM-1::GFP* had a greater effect on the anterior VPCs than on the posterior VPCs. To test whether this activity of *cam-1* requires the intracellular domain, we expressed a version of *CAM-1::GFP* lacking the intracellular domain (*CAM-1ΔIntra::GFP*) in muscle. *Pmyo-3::CAM-1ΔIntra::GFP* caused a UI phenotype, indicating that the intracellular domain is not required. This observation is consistent with our analysis of *cam-1* mutant alleles. Although expressed at levels similar to the other transgenes, based on GFP expression, neither *Psur-2::CAM-1::GFP*, *Plst-1::CAM-1::GFP*, *Pdpy-8::CAM-1::GFP* nor *Pfos-1a::CAM-1::GFP* caused a UI phenotype. These CAM-1 overexpression experiments indicate that CAM-1 can non-autonomously inhibit vulval induction. Because our analysis of *cam-1* mutant alleles suggested that the CAM-1 CRD is necessary to inhibit vulval induction, we tested whether overexpression of the membrane-tethered CAM-1 CRD is sufficient to inhibit vulval induction. The *cwEx164* transgene expresses *CAM-1::GFP* lacking the intracellular domain and the extracellular immunoglobulin and kringle domains (*CAM-1Δ IgKriIntra::GFP*) (Kim and Forrester, 2003). *Pcam-1::CAM-1ΔIgKriIntra::GFP* was sufficient to cause frequent fusion of P3.p and P4.p and to cause occasional F or 3° fates in P5.p. The mild effects on P5.p fate caused by *Pcam-1::CAM-1ΔIgKriIntra::GFP* compared with other transgenes could be due to less robust expression under *Pcam-1* or to instability of the severely truncated protein.

Loss of any single Wnt causes only minor induction defects (Gleason et al., 2006) (Table 1); therefore, *Pmyo-3::CAM-1::GFP* and *Psnb-1::CAM-1::GFP* are likely to interfere with multiple

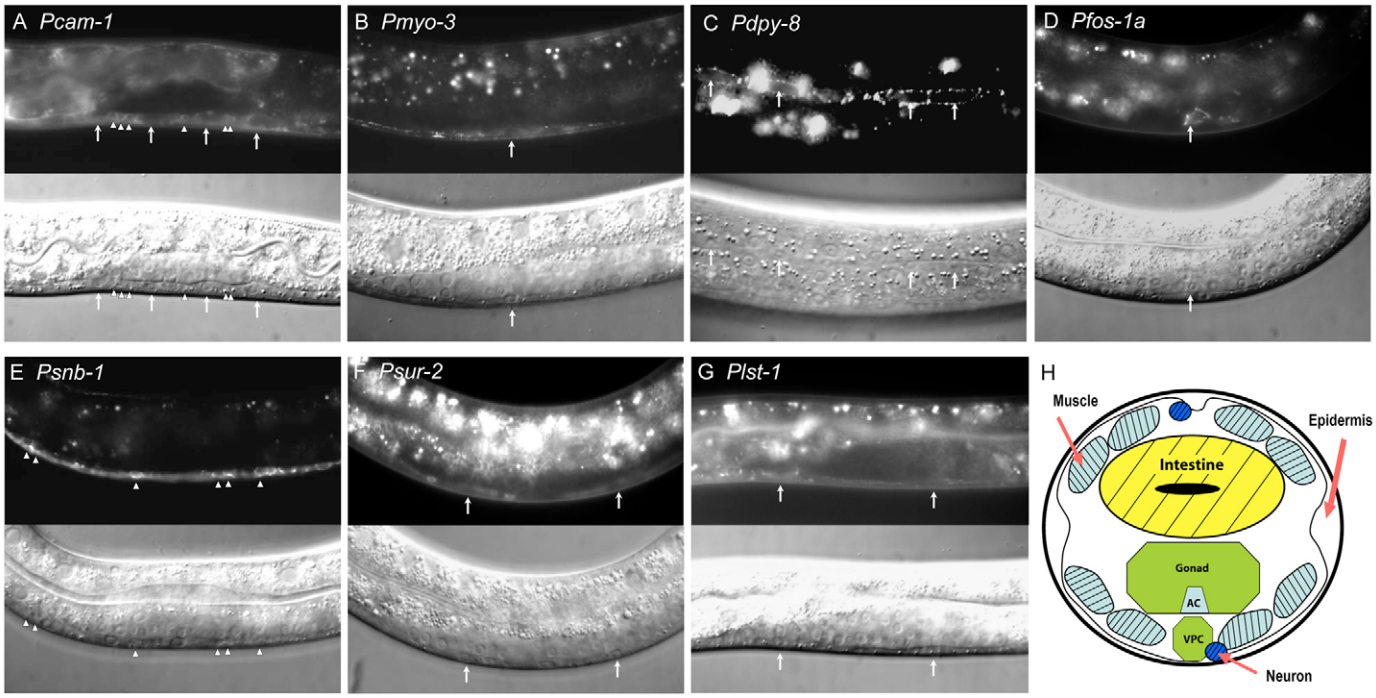


**Fig. 3. Transgene expression and worm cross-section.** Fluorescent (top) and Nomarski (bottom) images of animals carrying *CAM-1::GFP* translational fusions. Anterior, left; posterior, right. (**A**) *CAM-1::GFP* driven by the *cam-1* promoter. Membrane-localized expression is seen here in the ventral cord neurons (arrowheads) and VPCs (arrows). (**B**) *Pmyo-3::CAM-1::GFP* is expressed in body wall muscle (arrow). (**C**) *Pdpy-8::CAM-1::GFP* is expressed in the hypodermis. Arrows point to hypodermal seam cell nuclei. (**D**) *Pfos-1a::CAM-1::GFP* is expressed in the AC (arrow). (**E**) *Psnb-1::CAM-1::GFP* is expressed in nervous tissue. Expression shown here is in VCNs (arrowheads). (**F**) *Psur-2::CAM-1::GFP* is expressed in the VPCs (arrows) and in a few VCNs. (**G**) *Plst-1::CAM-1::GFP* is expressed in the VPCs (arrows). (**H**) Schematic cross-section of *C. elegans* hermaphrodite at the vulva. Major tissues are labeled, hatched areas represent sites of *cwn-1* and *cwn-2* expression.

**Table 2. Overexpression of CAM-1 in muscle or neurons inhibits vulval development in a Wnt-dependent manner**

| Relevant genotype* | % F fates: 3° fates: induced fates observed | | | | | | | |
|---|---|---|---|---|---|---|---|---|
| | P3.p | P4.p | P5.p | P6.p | P7.p | P8.p | % UI† | *n* |
| + | 58:42:0 | 0:100:0 | 0:0:100 | 0:0:100 | 0:0:100 | 0:100:0 | 0 | 62 |
| *bar-1(ga80)* | 100:0:0 | 91:7:2 | 39:7:54 | 10:0:90 | 12:8:80 | 36:62:2 | **64** | 59 |
| *cam-1(gm122)* | 23:77:0 | 0:100:0 | 0:0:100 | 0:0:100 | 0:0:100 | 0:100:0 | 0 | 34 |
| *cwn-1(ok546); egl-20(n585)* | 100:0:0 | 87:13:0 | 69:10:21 | 13:10:77 | 21:10:69 | 46:54:0 | **85** | 39 |
| *cwn-1(ok546); cwn-2(ok895)* | 91:9:0 | 75:25:0 | 23:2:75 | 2:0:98 | 2:0:98 | 2:98:0 | **27** | 44 |
| *syEx778[Pmyo-3::CAM-1::GFP]* | 95:5:0 | 67:33:0 | 29:5:66 | 5:0:95 | 0:0:100 | 0:100:0 | **29** | 21 |
| *syEx781[Pmyo-3::CAM-1::GFP]* | 76:24:0 | 40:60:0 | 16:8:76 | 0:0:100 | 0:0:100 | 4:96:0 | **28** | 25 |
| *syEx798[Pdpy-8::CAM-1::GFP]* | 65:35:0 | 5:95:0 | 0:0:100 | 0:0:100 | 0:0:100 | 0:100:0 | 0 | 20 |
| *syEx799[Pdpy-8::CAM-1::GFP]* | 65:35:0 | 0:100:0 | 0:0:100 | 0:0:100 | 0:0:100 | 0:100:0 | 0 | 20 |
| *syEx780[Pfos-1a::CAM-1::GFP]* | 38:62:0 | 0:100:0 | 0:0:100 | 0:0:100 | 0:0:100 | 0:100:0 | 0 | 21 |
| *syEx777[Pfos-1a::CAM-1::GFP]* | 76:24:0 | 5:95:0 | 0:0:100 | 0:0:100 | 0:0:100 | 0:100:0 | 0 | 21 |
| *syEx775[Psnb-1::CAM-1::GFP]* | 82:18:0 | 45:55:0 | 18:0:82 | 5:0:95 | 5:0:95 | 9:91:0 | **27** | 22 |
| *syEx776[Psnb-1::CAM-1::GFP]* | 55:45:0 | 14:86:0 | 5:0:95 | 0:0:100 | 0:0:100 | 5:95:0 | **5** | 22 |
| *syEx863[Psur-2::CAM-1::GFP]* | 23:77:0 | 0:95:5** | 0:0:100 | 0:0:100 | 0:5:95 | 0:100:0 | 0 | 20 |
| *syEx864[Psur-2::CAM-1::GFP]* | 15:85:0 | 0:100:0 | 0:0:100 | 0:0:100 | 0:0:100 | 0:100:0 | 0 | 22 |
| *syIs198[Plst-1::CAM-1::GFP]* | 23:77:0 | 0:100:0 | 0:0:100 | 0:0:100 | 0:0:100 | 0:100:0 | 0 | 22 |
| *syEx814[Pmyo-3::CAM-1ΔIntra::GFP]* | 100:0:0 | 75:25:0 | 20:0:80 | 0:10:90 | 5:0:95 | 0:100:0 | **20** | 20 |
| *cwEx164[Pcam-1::CAM-1ΔIgKriIntra::GFP]* | 91:9:0 | 59:41:0 | 5:5:91 | 0:0:100 | 0:0:100 | 5:95:0 | **9** | 22 |
| *cwn-2(ok895); syEx778[Pmyo-3::CAM-1::GFP]* | 100:0:0 | 84:12:4 | 40:36:24 | 4:8:88 | 12:4:84 | 36:64:0 | **88**‡ | 25 |
| *cwn-1(ok546); syEx778[Pmyo-3::CAM-1::GFP]* | 100:0:0 | 70:25:5 | 40:0:60 | 0:0:100 | 5:15:80 | 30:70:0 | **40**§ | 20 |
| *egl-20(n585); syEx778[Pmyo-3::CAM-1::GFP]* | 95:5:0 | 95:5:0 | 50:0:50 | 15:0:85 | 10:10:80 | 70:30:0 | **60**¶ | 20 |

Strains containing *syEx* transgenes were grown at 25°C; all other strains were grown at 20°C.
**syEx* transgenic lines carry *unc-119(ed4); him-5(e1490)* and an *unc-119(+)* rescuing plasmid. *dpy-20(e1282)* was used to suppress the roller phenotype of *cwEx164*, which was co-injected with pRF4.
†% underinduced. Percentage of animals that have fewer than three VPCs induced. Bold indicates occurrence of underinduction.
‡$P<0.0001$, §$P>0.05$, ¶$P=0.026$ compared with *syEx778* using Fisher's exact test.
**The occurrence of an induced fate here represents an animal where the vulva was shifted anteriorly, but was not overinduced.

Wnts. To determine with which Wnts *CAM-1::GFP* interferes, we analyzed *Pmyo-3::CAM-1::GFP* in worms mutant for *cwn-1*, *egl-20* and *cwn-2*, the three Wnts contributing most to VPC induction (Table 2). Loss of a Wnt that retains inductive activity in a *Pmyo-3::CAM-1::GFP* background should display enhancement of the UI phenotype, whereas loss of a Wnt that is already fully antagonized by *Pmyo-3::CAM-1::GFP* should not enhance the phenotype. Both *egl-20(rf)* and *cwn-2(lf)* significantly enhanced the UI phenotype of *Pmyo-3::CAM-1::GFP* (Table 2), indicating that these Wnts retain some or all of their inductive activity. By contrast, we found that mutation of *cwn-1* did not significantly enhance the UI phenotype, indicating that the inductive activity of CWN-1 is largely abrogated by *Pmyo-3::CAM-1::GFP*.

## DISCUSSION

Despite studies in several different organisms, the mechanism of ROR action remains elusive. In this work, we characterized the role of CAM-1/ROR as a regulator of Wnt distribution and determined that one function of ROR proteins is to sequester Wnts (Fig. 4).

Previously, it was hypothesized that CAM-1/ROR could sequester Wnts. Kim and Forrester (Kim and Forrester, 2003) found that expression of the membrane-anchored CAM-1 ECD was sufficient to rescue the cell migration defects of *cam-1(lf)* worms and that overexpression of the membrane-anchored CAM-1 CRD caused defects in HSN and Q cell migration similar to those caused by mutation of *egl-20/Wnt*, leading these authors to propose that the CAM-1 CRD might sequester EGL-20/WNT. Indeed, CAM-1 was later shown to inhibit EGL-20 signaling in cell migration independently of the CAM-1 cytoplasmic domain (Forrester et al., 2004). However, the mechanism of this inhibition was not demonstrated. In particular, as the ROR2 CRD is capable of dimerizing with Fz (Oishi et al., 2003), the CAM-1 ECD could potentially function cell-autonomously by inhibiting the Wnt receptor.

The genetic data presented here indicate that CAM-1 antagonizes Wnt signaling during vulval development. We found that in *lin-17* and *lin-18* mutant backgrounds, *cam-1* mutations cause an OI phenotype owing to elevated levels of Wnt activity. Loss of *lin-17* or *lin-18* might provide a sensitized background if LIN-17 and LIN-18, like CAM-1, also affect the extracellular distribution of Wnts.

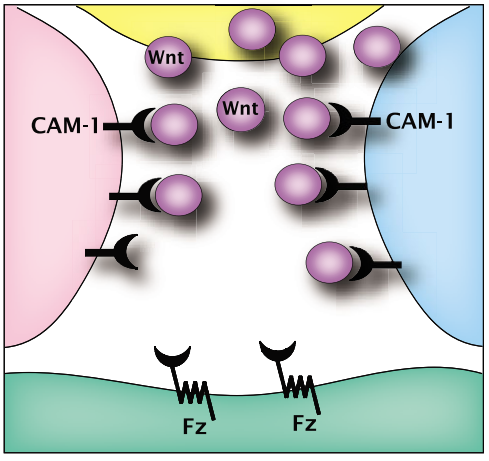


**Fig. 4. Model for CAM-1 sequestation of Wnts in *C. elegans*.** CAM-1 expressed in tissues between the source of Wnt expression and the recipient tissue can sequester Wnt by direct binding to the CRD and can thereby limit the amount of Wnt reaching the recipient tissue.

According to this hypothesis, mutation of *lin-17* or *lin-18* would similarly result in elevated extracellular Wnt levels; however, our data do not conclusively support this hypothesis.

Using vulval development as a model, we showed conclusively that CAM-1/ROR can act non-autonomously. The source of the Wnts required for vulval induction is unknown and a sequestration model would require that *Pmyo-3::CAM-1::GFP* (muscle expression) and *Psnb-1::CAM-1::GFP* (neuronal expression) are expressed in positions that enable them to restrict diffusion or transport of the Wnts to the VPCs (Fig. 3H). EGL-20/WNT forms a gradient of decreasing concentration from its site of expression in the tail extending anteriorly past the VPCs (Coudreuse et al., 2006). The distance between the source of EGL-20 and the VPCs provides ample opportunity for CAM-1 expressed in nervous or muscle tissue to prevent EGL-20 from reaching the VPCs. CWN-1/WNT is expressed in ventral cord neurons (VCNs) and posterior body wall muscle (Gleason et al., 2006; Hilliard and Bargmann, 2006). Endogenous CAM-1 expression in body wall muscle and VCNs, which are in close proximity to the VPCs (Fig. 3H), could place CAM-1 between the source of *cwn-1* expression and the VPCs, allowing CAM-1 to act as a barrier and limit the amount of Wnt signal received by the VPCs (Fig. 4). CAM-1 could also function at the Wnt source to limit secretion. Consistent with inhibition by sequestration, CAM-1 overexpression antagonizes Wnt signaling independently of the cytoplasmic domain. Also, phenotypes of *cam-1* mutants indicate that the membrane-anchored ECD is sufficient to inhibit Wnt signaling.

A sequestration model also predicts that CAM-1 specifically binds to those Wnts that it antagonizes. In agreement with our genetic data, we found that the CAM-1 CRD can bind to Wnts CWN-1, EGL-20 and MOM-2 in vitro. Our initial experimental design included measuring binding at various concentrations of CRD-AP that would allow us to calculate the binding affinity of each receptor-ligand pair. However, our preliminary results showed high background binding to untransfected S2 cells. We thus chose the concentration of CRD-AP at which we saw the greatest difference between binding to Nrt-Wnt-expressing and to untransfected cells and tested all of the combinations at this concentration in triplicate. Wu and Nusse (Wu and Nusse, 2002) reported that the binding of DFz2CRD-AP to Nrt-Wg-expressing cells was 10-fold higher than to untransfected cells. In our experiments, we never observed a difference greater than 2-fold. Weaker binding could be caused by a species barrier, whereby the *Drosophila* cells do not express a necessary cofactor or do not process Wnts in a manner conducive to high-affinity binding to *C. elegans* receptors. Although the binding we detected is not as robust as that observed for *Drosophila* Wnts and Fzs, we feel that it might still be informative and have included these values in a supplementary table (see Table S3 in the supplementary material).

Although sequestration through Wnt-CRD binding can account for many functions of CAM-1/ROR, there are examples in which CAM-1 might function by a different mechanism. The membrane-anchored ECD, but not the membrane-anchored CRD alone, was sufficient to rescue all cell migration defects of *cam-1(lf)* worms (Kim and Forrester, 2003). In cases where the CRD was not sufficient, ligand binding might require additional CAM-1 ECD(s) – e.g. the kringle or Ig domain – or these might be cases in which CAM-1 functions by a non-sequestration mechanism. Other examples of CAM-1 function that are probably not due to sequestration include cell-autonomous roles in CAN migration (Forrester et al., 1999) and development of the ASI sensory neuron (Koga et al., 1999). Also, CAM-1 function in Pn.aap division orientation in males requires CAM-1 kinase activity (Forrester et al., 1999; Kim and Forrester, 2003). Although our study has furthered our understanding of ROR function, the role of the cytoplasmic domains remains elusive. CAM-1 shares 44% identity in the kinase domain to human ROR1 and ROR2 and none of the 21 invariant amino acids is altered (Forrester, 2002). Although ROR proteins have demonstrated kinase activity (Masiakowski and Carroll, 1992; Oishi et al., 1999), the precise function of this activity has not been identified.

Our genetic and biochemical observations that CAM-1 interacts not only with EGL-20, but also with other Wnts, suggest that CAM-1 is an important general regulator of Wnt activity, rather than a specific EGL-20 antagonist. As a system in which neighboring cells reproducibly adopt distinct fates, vulva induction has enabled us to study how CAM-1 affects the precision of Wnt distribution. The subtle effects we observed upon *cam-1* manipulation suggest that CAM-1 serves to buffer Wnt levels rather than to dramatically affect Wnt localization. Such buffering mechanisms might provide robustness to the Wnt morphogen gradient. The high degree of similarity between CAM-1 and vertebrate ROR proteins (Forrester, 2002), in addition to the ability of ROR proteins to inhibit Wnt signaling in a kinase-independent manner, suggest a conserved function of ROR proteins to fine-tune the spatial profile of Wnt activity and to help create regions of distinct cell fate in complex multicellular organisms.

We thank Gladys Medina and Barbara Perry for technical assistance and members of the Sternberg laboratory for helpful discussions. For reagents and worms we thank W. Forrester, C. Wu, A. Fire, A. V. Maricq, M. Francis, D. Sherwood, I. Greenwald and H. Sawa. Some Nematode strains were from the *Caenorhabditis* Genetics Center, funded by the NIH National Center for Research Resources. We thank Cheryl Van Buskirk, Ryan Baugh, Jagan Srinivasan and Mihoko Kato for critically reading the manuscript; the Benzer laboratory (especially Gil Carvallo) for use of their microplate spectrophotometer; the Hay laboratory for use of their tissue culture hood; Jost Vielmetter and Inderjit Nangiana of the Caltech Protein Expression Facility for production of CRD-AP conditioned media; and Julie Gleason for kindly exchanging *lin-17* and *mom-5* mutant alleles. P.W.S. is an investigator with the Howard Hughes Medical Institute and J.L.G. was supported by the Thomas Hunt Morgan Fellowship for graduate study toward the doctor of philosophy degree in biology at the California Institute of Technology.

**Supplementary material**

Supplementary material for this article is available at
http://dev.biologists.org/cgi/content/full/134/22/4053/DC1

**References**

**Ailion, M. and Thomas, J. H.** (2003). Isolation and characterization of high-temperature-induced Dauer formation mutants in Caenorhabditis elegans. *Genetics* **165**, 127-144.

**Bhanot, P., Brink, M., Samos, C. H., Hsieh, J. C., Wang, Y., Macke, J. P., Andrew, D., Nathans, J. and Nusse, R.** (1996). A new member of the frizzled family from Drosophila functions as a Wingless receptor. *Nature* **382**, 225-230.

**Billiard, J., Way, D. S., Seestaller-Wehr, L. M., Moran, R. A., Mangine, A. and Bodine, P. V.** (2005). The orphan receptor tyrosine kinase Ror2 modulates canonical Wnt signaling in osteoblastic cells. *Mol. Endocrinol.* **19**, 90-101.

**Brenner, S.** (1974). The genetics of Caenorhabditis elegans. *Genetics* **77**, 71-94.

**Cheng, H. J. and Flanagan, J. G.** (1994). Identification and cloning of ELF-1, a developmentally expressed ligand for the Mek4 and Sek receptor tyrosine kinases. *Cell* **79**, 157-168.

**Coudreuse, D. Y., Roel, G., Betist, M. C., Destree, O. and Korswagen, H. C.** (2006). Wnt gradient formation requires retromer function in Wnt-producing cells. *Science* **312**, 921-924.

**Davies, A. G., Pierce-Shimomura, J. T., Kim, H., VanHoven, M. K., Thiele, T. R., Bonci, A., Bargmann, C. I. and McIntire, S. L.** (2003). A central role of the BK potassium channel in behavioral responses to ethanol in C. elegans. *Cell* **115**, 655-666.

**Eisenmann, D. M.** (2005). Wnt Signaling. In *Wormbook* (ed. The *C. elegans* Research Community), Wormbook, doi/10.1895/wormbook.1.7.1, http://www.wormbook.org.

**Eisenmann, D. M., Maloof, J. N., Simske, J. S., Kenyon, C. and Kim, S. K.**

(1998). The beta-catenin homolog BAR-1 and LET-60 Ras coordinately regulate the Hox gene lin-39 during Caenorhabditis elegans vulval development. *Development* **125**, 3667-3680.
**Ferguson, E. L. and Horvitz, H. R.** (1985). Identification and characterization of 22 genes that affect the vulval cell lineages of the nematode Caenorhabditis elegans. *Genetics* **110**, 17-72.
**Ferguson, E. L., Sternberg, P. W. and Horvitz, H. R.** (1987). A genetic pathway for the specification of the vulval cell lineages of Caenorhabditis elegans. *Nature* **326**, 259-267.
**Flanagan, J. G. and Leder, P.** (1990). The kit ligand: a cell surface molecule altered in steel mutant fibroblasts. *Cell* **163**, 185-194.
**Forrester, W. C.** (2002). The Ror receptor tyrosine kinase family. *Cell. Mol. Life Sci.* **59**, 83-96.
**Forrester, W. C., Perens, E., Zallen, J. A. and Garriga, G.** (1998). Identification of Caenorhabditis elegans genes required for neuronal differentiation and migration. *Genetics* **148**, 151-165.
**Forrester, W. C., Dell, M., Perens, E. and Garriga, G.** (1999). A C. elegans Ror receptor tyrosine kinase regulates cell motility and asymmetric cell division. *Nature* **400**, 881-885.
**Forrester, W. C., Kim, C. and Garriga, G.** (2004). The Caenorhabditis elegans Ror RTK CAM-1 inhibits EGL-20/Wnt signaling in cell migration. *Genetics* **168**, 1951-1962.
**Francis, M. M., Evans, S. P., Jensen, M., Madsen, D. M., Mancuso, J., Norman, K. R. and Maricq, A. V.** (2005). The Ror receptor tyrosine kinase CAM-1 is required for ACR-16-mediated synaptic transmission at the C. elegans neuromuscular junction. *Neuron* **46**, 581-594.
**Gill, G. and Ptashne, M.** (1988). Negative effect of the transcriptional activator GAL4. *Nature* **334**, 721-724.
**Gleason, J. E., Korswagen, H. C. and Eisenmann, D. M.** (2002). Activation of Wnt signaling bypasses the requirement for RTK/Ras signaling during C. elegans vulval induction. *Genes Dev.* **16**, 1281-1290.
**Gleason, J. E., Szyleyko, E. A. and Eisenmann, D. M.** (2006). Multiple redundant Wnt signaling components function in two processes during C. elegans vulval development. *Dev. Biol.* **298**, 442-457.
**Greenwald, I. S., Sternberg, P. W. and Horvitz, H. R.** (1983). The lin-12 locus specifies cell fates in Caenorhabditis elegans. *Cell* **34**, 435-444.
**Han, C., Yan, D., Belenkaya, T. Y. and Lin, X.** (2005). Drosophila glypicans Dally and Dally-like shape the extracellular Wingless morphogen gradient in the wing disc. *Development* **132**, 667-679.
**Han, M. and Sternberg, P. W.** (1990). let-60, a gene that specifies cell fates during C. elegans vulval induction, encodes a ras protein. *Cell* **63**, 921-931.
**Harris, J., Honigberg, L., Robinson, N. and Kenyon, C.** (1996). Neuronal cell migration in C. elegans: regulation of Hox gene expression and cell position. *Development* **122**, 3117-3131.
**Hikasa, H., Shibata, M., Hiratani, I. and Taira, M.** (2002). The Xenopus receptor tyrosine kinase Xror2 modulates morphogenetic movements of the axial mesoderm and neuroectoderm via Wnt signaling. *Development* **129**, 5227-5239.
**Hill, R. J. and Sternberg, P. W.** (1992). The gene lin-3 encodes an inductive signal for vulval development in C. elegans. *Nature* **358**, 470-476.
**Hilliard, M. A. and Bargmann, C. I.** (2006). Wnt signals and frizzled activity orient anterior-posterior axon outgrowth in C. elegans. *Dev. Cell* **10**, 379-390.
**Hopper, N. A., Lee, J. and Sternberg, P. W.** (2000). ARK-1 inhibits EGFR signaling in C. elegans. *Mol. Cell* **6**, 65-75.
**Inoue, T., Oz, H. S., Wiland, D., Gharib, S., Deshpande, R., Hill, R. J., Katz, W. S. and Sternberg, P. W.** (2004). C. elegans LIN-18 is a Ryk ortholog and functions in parallel to LIN-17/Frizzled in Wnt signaling. *Cell* **118**, 795-806.
**Kani, S., Oishi, I., Yamamoto, H., Yoda, A., Suzuki, H., Nomachi, A., Iozumi, K., Nishita, M., Kikuchi, A., Takumi, T. et al.** (2004). The receptor tyrosine kinase Ror2 associates with and is activated by casein kinase Iepsilon. *J. Biol. Chem.* **279**, 50102-50109.
**Katz, W. S., Hill, R. J., Clandinin, T. R. and Sternberg, P. W.** (1995). Different levels of the C. elegans growth factor LIN-3 promote distinct vulval precursor fates. *Cell* **82**, 297-307.
**Kawano, Y. and Kypta, R.** (2003). Secreted antagonists of the Wnt signalling pathway. *J. Cell Sci.* **116**, 2627-2634.
**Kim, C. and Forrester, W. C.** (2003). Functional analysis of the domains of the C elegans Ror receptor tyrosine kinase CAM-1. *Dev. Biol.* **264**, 376-390.
**Kimble, J.** (1981). Alterations in cell lineage following laser ablation of cells in the somatic gonad of Caenorhabditis elegans. *Dev. Biol.* **87**, 286-300.
**Koga, M., Take-uchi, M., Tameishi, T. and Ohshima, Y.** (1999). Control of DAF-7 TGF-(alpha) expression and neuronal process development by a receptor tyrosine kinase KIN-8 in Caenorhabditis elegans. *Development* **126**, 5387-5398.
**Korswagen, H. C., Coudreuse, D. Y., Betist, M. C., van de Water, S., Zivkovic, D. and Clevers, H. C.** (2002). The Axin-like protein PRY-1 is a negative regulator of a canonical Wnt pathway in C. elegans. *Genes Dev.* **16**, 1291-1302.
**Logan, C. Y. and Nusse, R.** (2004). The Wnt signaling pathway in development and disease. *Annu. Rev. Cell Dev. Biol.* **20**, 781-810.
**Masiakowski, P. and Carroll, R. D.** (1992). A novel family of cell surface receptors with tyrosine kinase-like domain. *J. Biol. Chem.* **267**, 26181-26190.
**Mello, C. C., Kramer, J. M., Stinchcomb, D. and Ambros, V.** (1991). Efficient gene transfer in C. elegans: extrachromosomal maintenance and integration of transforming sequences. *EMBO J.* **10**, 3959-3970.
**Mikels, A. J. and Nusse, R.** (2006a). Purified Wnt5a protein activates or inhibits beta-Catenin-TCF signaling depending on receptor context. *PLoS Biol.* **4**, e115.
**Mikels, A. J. and Nusse, R.** (2006b). Wnts as ligands: processing, secretion and reception. *Oncogene* **25**, 7461-7468.
**Nonet, M. L., Saifee, O., Zhao, H., Rand, J. B. and Wei, L.** (1998). Synaptic transmission deficits in Caenorhabditis elegans synaptobrevin mutants. *J. Neurosci.* **18**, 70-80.
**Oishi, I., Takeuchi, S., Hashimoto, R., Nagabukuro, A., Ueda, T., Liu, Z. J., Hatta, T., Akira, S., Matsuda, Y., Yamamura, H. et al.** (1999). Spatio-temporally regulated expression of receptor tyrosine kinases, mRor1, mRor2, during mouse development: implications in development and function of the nervous system. *Genes Cells* **4**, 41-56.
**Oishi, I., Suzuki, H., Onishi, N., Takada, R., Kani, S., Ohkawara, B., Koshida, I., Suzuki, K., Yamada, G., Schwabe, G. C. et al.** (2003). The receptor tyrosine kinase Ror2 is involved in non-canonical Wnt5a/JNK signalling pathway. *Genes Cells* **8**, 645-654.
**Okkema, P. G., Harrison, S. W., Plunger, V., Aryana, A. and Fire, A.** (1993). Sequence requirements for myosin gene expression and regulation in Caenorhabditis elegans. *Genetics* **135**, 385-404.
**Rulifson, E. J., Wu, C. H. and Nusse, R.** (2000). Pathway specificity by the bifunctional receptor frizzled is determined by affinity for wingless. *Mol. Cell* **6**, 117-126.
**Savage-Dunn, C.** (2005). TGF-β signaling. In *Wormbook* (ed. The *C. elegans* Research Community), Wormbook, doi/10.1895/wormbook.1.22.1, http://ww.wormbook.org.
**Sawa, H., Lobel, L. and Horvitz, H. R.** (1996). The Caenorhabditis elegans gene lin-17, which is required for certain asymmetric cell divisions, encodes a putative seven-transmembrane protein similar to the Drosophila frizzled protein. *Genes Dev.* **10**, 2189-2197.
**Sherwood, D. R. and Sternberg, P. W.** (2003). Anchor cell invasion into the vulval epithelium in C. elegans. *Dev. Cell* **5**, 21-31.
**Simske, J. S. and Kim, S. K.** (1995). Sequential signalling during Caenorhabditis elegans vulval induction. *Nature* **375**, 142-146.
**Singh, N. and Han, M.** (1995). sur-2, a novel gene, functions late in the let-60 ras-mediated signaling pathway during Caenorhabditis elegans vulval induction. *Genes Dev.* **9**, 2251-2265.
**Sternberg, P. W.** (2005). Vulval development. In *Wormbook* (ed. The *C. elegans* Research Community), Wormbook, doi/10.1895/wormbook.1.6.1, http://ww.wormbook.org.
**Sternberg, P. W. and Horvitz, H. R.** (1989). The combined action of two intercellular signaling pathways specifies three cell fates during vulval induction in C. elegans. *Cell* **58**, 679-693.
**Sullivan, D. T., MacIntyre, R., Fuda, N., Fiori, J., Barrilla, J. and Ramizel, L.** (2003). Analysis of glycolytic enzyme co-localization in Drosophila flight muscle. *J. Exp. Biol.* **206**, 2031-2038.
**Sulston, J. E. and Horvitz, H. R.** (1977). Post-embryonic cell lineages of the nematode, Caenorhabditis elegans. *Dev. Biol.* **56**, 110-156.
**Sulston, J. E. and White, J. G.** (1980). Regulation and cell autonomy during postembryonic development of Caenorhabditis elegans. *Dev. Biol.* **78**, 577-597.
**Sundaram, M. V.** (2006). RTK/Ras/MAPK signaling. In *Wormbook* (ed. The *C. elegans* Research Community), Wormbook, doi/10.1895/wormbook.1.80.1, http://ww.wormbook.org.
**Tan, P. B., Lackner, M. R. and Kim, S. K.** (1998). MAP kinase signaling specificity mediated by the LIN-1 Ets/LIN-31 WH transcription factor complex during C. elegans vulval induction. *Cell* **93**, 569-580.
**Wu, C. H. and Nusse, R.** (2002). Ligand receptor interactions in the Wnt signaling pathway in Drosophila. *J. Biol. Chem.* **277**, 41762-41769.
**Yoo, A. S., Bais, C. and Greenwald, I.** (2004). Crosstalk between the EGFR and LIN-12/Notch pathways in C. elegans vulval development. *Science* **303**, 663-666.
**Yoon, C. H., Chang, C., Hopper, N. A., Lesa, G. M. and Sternberg, P. W.** (2000). Requirements of multiple domains of SLI-1, a Caenorhabditis elegans homologue of c-Cbl, and an inhibitory tyrosine in LET-23 in regulating vulval differentiation. *Mol. Biol. Cell* **11**, 4019-4031.

**Table S1. *cam-1* genetically interacts with known regulators of vulval induction**

| Relevant genotype* | Average no. of VPCs induced | *n* | *P* value† |
|---|---|---|---|
| *bar-1(ga80)* | 1.50±0.29 | 50 | |
| *cam-1(gm122); bar-1(ga80)* | 1.45±0.13 | 52 | Not sig.‡ |
| *lin-3(e1417)* | 0.28±0.16 | 20 | |
| *cam-1(gm122); lin-3(e1417)* | 0.76±0.20 | 21 | 0.04§ |
| *lin-3(n378)* | 0.78±0.19 | 32 | |
| *cam-1(gm122); lin-3(n378)* | 1.68±0.23 | 20 | 0.007§ |
| *cam-1(gm122)* | 3.01±0.01 | 55 | |
| *cam-1(gm122); ark-1(sy247)* | 3.00±0.00 | 21 | Not sig.¶ |
| *cam-1(gm122); sli-1(sy143)* | 3.05±0.03 | 22 | Not sig.¶ |
| *cam-1(gm122); gap-1(n1691)* | 3.05±0.05 | 22 | Not sig.¶ |
| *lin-17(n671); gap-1(n1691)* | 3.00±0.00 | 22 | Not sig.** |
| *lin-12(n952/+)* | 0.87±0.14 | 63 | |
| *cam-1(gm122); lin-12(n952/+)* | 1.85±0.24 | 34 | 0.001†† |
| *lin-17(n671); cam-1(gm122); daf-3(mgDf90)* | 3.14±0.08 | 21 | Not sig.‡‡ |

Worms were grown and scored 20°C. Induced values are mean±s.e.m.

**gap-1(n1691)* linked to *unc-2(e55)*, *ark-1(sy247)* linked to *dpy-20(e1282). cam-1(gm122); lin-12(n952)* male worms were crossed into *cam-1(gm122); rol-6(e187)* and non-roller F1s were scored.

†*P* values were calculated using Mann-Whitney two-tailed test. *P*<0.05 considered significant.

‡Compared with *bar-1(ga80)* alone; §compared with *lin-3(rf)* alone; ¶compared with *cam-1(gm122)* alone; **compared with *lin-17(n671)* alone; ††compared with *lin-12(n952/+)*; ‡‡compared with *cam-1(gm122); lin-17(n671)*.

**Table S2. Contribution of Wnt receptors MOM-5, LIN-17 and LIN-18 to vulval induction**

| Genotype | % OI* | % UI† | Average no. of VPCs induced | *n* |
|---|---|---|---|---|
| + | 0 | 0 | 3 | Many |
| *lin-17(n671)* | 0 | 0 | 3±0.00 | 113 |
| *lin-18(e620)* | 0 | 0 | 3±0.00 | 113 |
| *lin-17(n671); lin-18(e620)* | 2 | 0 | 3.02±0.02§ | 51 |
| *syIs75[LIN-18::GFP]* | 0 | 13 | 2.97±0.02 | 53 |
| *cwn-1(ok546)* | 0 | 13 | 2.87±0.04 | 62 |
| *cwn-1(ok546); syIs75[LIN-18::GFP]* | 0 | 21 | 2.68±0.11¶ | 53 |
| *syEx1022[LIN-17::GFP]* | 0 | 0 | 3.00±0.00 | 53 |
| *cwn-1(ok546); syEx1022[LIN-17::GFP]* | 0 | 28 | 2.72±0.09 | 25 |
| *syEx1020[Pmyo-3::LIN-17::GFP]* | 0 | 3 | 2.99±0.01 | 39 |
| *cwn-1(ok546); syEx1020[Pmyo-3::LIN-17::GFP]* | 0 | 15 | 2.85±0.08 | 20 |
| *lin-17(n671)-DE*‡ | 2 | 0 | 3.04±0.04** | 51 |
| *lin-17(n671)-DE*‡*; cam-1(gm122)* | 10 | 2 | 3.07±0.05 | 50 |
| *mom-5(zu193)* | 0 | 49 | 2.52±0.07†† | 51 |
| *mom-5(zu193)-DE*‡ | 2 | 39 | 2.63±0.07†† | 56 |
| *mom-5(or57)* | 0 | 67 | 2.26±0.08†† | 52 |
| *lin-17(n677)* | 5 | 0 | 3.05±0.05 | 22 |
| *lin-17(n677); cam-1(gm122)* | 18 | 0 | 3.11±0.06 | 22 |
| *mig-1(e1787); lin-17(n671)* | 5 | 0 | 3.02±0.02 | 23 |
| *lin-17(n671); cfz-2(ok1201)* | 5 | 0 | 3.02±0.03 | 22 |
| *lin-17(n671); cwn-1(ok546)* | 0 | 7 | 2.93±0.03 | 58 |

Worms were grown and scored at 20°C. Induced values are mean±s.e.m.

*Overinduced animals are those with greater than three VPCs induced.

†Underinduced animals are those with less than 3 VPCs induced.

‡These strains were obtained from the Eisenmann laboratory and were compared to strains from the Sternberg laboratory.

§1/51 *lin-17(n671); lin-18(e620)* double-mutant worms had 4 VPCs induced (see Fig. S1 in the supplementary material).

¶*syIs75* increased the fraction of *cwn-1(lf)* worms that had a more severe UI phenotype (less than 2 VPCs induced), $P$=0.04.

**1/51 *lin-17(n671)-DE* worms had 5 VPCs induced (see Fig. S1).

††*mom-5* mutant worms frequently had only 2 VPCs induced (see Fig. S1).

**Table S3. Binding assay raw data**

| CRD-AP | LIN-44 | CWN-1 | EGL-20 | CWN-2 | MOM-2 | S2 |
|---|---|---|---|---|---|---|
| MIG-1 | 0.177 | 0.163 | 0.236 | 0.158 | 0.205 | 0.169 |
| | 0.208 | 0.211 | 0.259 | 0.224 | 0.236 | 0.214 |
| | 0.233 | 0.181 | 0.199 | 0.210 | 0.260 | |
| Mean | **0.206** | **0.185** | **0.231** | **0.197** | **0.234** | **0.192** |
| LIN-17 | 0.166 | 0.158 | 0.193 | 0.218 | 0.151 | 0.172 |
| | 0.193 | 0.141 | 0.197 | 0.196 | 0.182 | 0.167 |
| | 0.257 | 0.210 | 0.236 | 0.211 | 0.143 | 0.141 |
| Mean | **0.205** | **0.170** | **0.209** | **0.208** | **0.159** | **0.160** |
| MOM-5 | 0.159 | 0.177 | 0.167 | 0.203 | 0.167 | 0.145 |
| | 0.148 | 0.287 | 0.174 | 0.151 | 0.185 | 0.179 |
| | 0.153 | 0.195 | 0.177 | 0.152 | 0.159 | |
| Mean | **0.153** | **0.220** | **0.173** | **0.169** | **0.170** | **0.162** |
| CAM-1 | 0.255 | 0.385 | 0.387 | 0.254 | 0.375 | 0.301 |
| | 0.276 | 0.370 | 0.421 | 0.263 | 0.382 | 0.206 |
| | 0.482 | 0.350 | 0.433 | 0.287 | 0.307 | 0.321 |
| Mean | **0.338** | **0.368** | **0.414** | **0.268** | **0.355** | **0.276** |
| CFZ-2 | 0.139 | 0.196 | 0.232 | 0.201 | 0.209 | 0.195 |
| | 0.166 | 0.192 | 0.200 | 0.187 | 0.198 | 0.129 |
| | 0.202 | 0.180 | 0.187 | 0.167 | 0.164 | |
| Mean | **0.169** | **0.189** | **0.206** | **0.185** | **0.190** | **0.162** |
| LIN-18 | 0.089 | 0.091 | 0.098 | 0.088 | 0.095 | 0.102 |
| | 0.093 | 0.092 | 0.097 | 0.109 | 0.099 | 0.089 |
| | | 0.125 | 0.090 | 0.087 | 0.093 | 0.101 |
| Mean | **0.091** | **0.103** | **0.095** | **0.095** | **0.096** | **0.097** |

Table lists 405 nm absorbance values after incubation of CRD-AP supernatant with the chromogenic substrate p-nitrophenyl phosphate (see Materials and methods for details).